Interfaces of Modulated Phases

Roland R. Netz,[1,2] David Andelman,[3] and M. Schick[1]

[1]*Department of Physics, University of Washington, Box 351560, Seattle, Washington 98195-1560*
[2]*Max-Planck-Institut für Kolloid- und Grenzflächenforschung, Kantstrasse 55, 14513 Teltow, Germany*
[3]*School of Physics and Astronomy, Tel-Aviv University, Ramat Aviv 69978, Tel Aviv, Israel*
(Received 22 November 1996)

Numerically minimizing a continuous free-energy functional which yields several modulated phases, we obtain the order-parameter profiles and interfacial free energies of symmetric and nonsymmetric tilt boundaries within the lamellar phase, and of interfaces between coexisting lamellar, hexagonal, and disordered phases. Our findings agree well with chevron, omega, and T-junction tilt-boundary morphologies observed in diblock copolymers and magnetic garnet films. [S0031-9007(97)03772-1]

Modulated phases are found in a surprisingly diverse set of physical and chemical systems, including superconductors, thin-film magnetic garnets and ferrofluids, Langmuir monolayers, and diblock copolymers [1]. Such phases are characterized by periodic spatial variations of the pertinent order parameter in the form of lamellae, cylinders, or cubic arrangements of spheres or interwoven sheets. This self-organization results from competing interactions: a short-ranged molecular one favoring a homogeneous state, and a long-ranged contribution, which can have a magnetic, electric, or elastic origin, favoring domains. Because of the modulation, interfaces between different phases or grain boundaries within a single phase are most interesting, yet they have received much less attention than those occurring in solids. Recently, experimental studies of grain boundaries within lamellar phases of diblock copolymer have been carried out [2,3] which illustrate the rich interfacial behavior exhibited by such systems. In particular, three morphologies of tilt boundaries [2(b)], denoted chevron, omega, and T-junction, were observed. Such interfaces are more difficult to describe theoretically than those between uniform phases, which have been the subject of classic work [4]. In this article we study not only tilt grain boundaries within lamellar phases but also interfaces between coexisting modulated phases of different symmetry.

The dimensionless free-energy functional we use,

$$\mathcal{F}[\phi] = \int \left\{ -\frac{\chi}{2}\phi^2 + \frac{1-\phi}{2}\ln\frac{1-\phi}{2} \right.$$
$$+ \frac{1+\phi}{2}\ln\frac{1+\phi}{2}$$
$$\left. - \frac{1}{2}(\nabla\phi)^2 + \frac{1}{2}(\nabla^2\phi)^2 - \mu\phi \right\} dV, \quad (1)$$

includes an enthalpic term (proportional to the interaction parameter χ) that favors an ordered state in which $|\phi|$ is nonzero, an entropy of mixing preferring a disordered state, $\phi = 0$, and confining $|\phi|$ to be less than unity, and derivatives of the order parameter. The ordered state occurs with a modulation of a dominant wave vector $q^* = 1/\sqrt{2}$ because of the competition between

the negative gradient square term (favoring domains at large length scales) and the positive Laplacian square (preferring a homogeneous state at small length scales). Such a free-energy functional has been used to describe the bulk phases of magnetic layers [5], Langmuir films [6], amphiphilic systems [7], diblock copolymers [8], and the effects of surfaces on isotropic [9] and hexagonal phases [10] of the latter.

In our numerical studies, we determine the minimum of (1) by *directly* using a conjugate-gradient method, which is more convenient than solving the corresponding Euler-Lagrange equation. We discretize ϕ on a square lattice, approximate the derivatives by nearest-neighbor differences, and employ a mesh size sufficiently small that discretization effects are negligible within the numerical precision. A typical grid contains 40 000 points. Figure 1 shows the resulting two-dimensional bulk phase diagram as a function of χ and (a) the average order parameter $\Phi \equiv \langle\phi\rangle_V$ and (b) the chemical potential μ. It is in good agreement with previous calculations based on single-mode approximations [5,6]. In addition to the disordered (D) phase, there is a lamellar (L) and two hexagonal
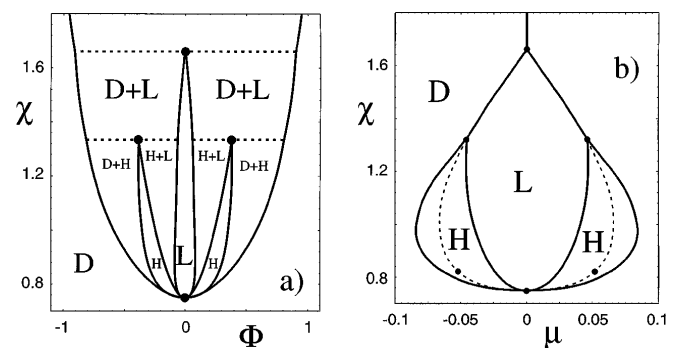

FIG. 1. Two-dimensional bulk phase diagram, showing disordered (D), lamellar (L), and hexagonal (H) phases, as a function of the interaction strength χ, and (a) the average order parameter Φ and (b) the chemical potential μ. Dashed lines in (a) denote triple lines and dashed lines in (b) denote the (metastable) L-D transitions which exhibit tricritical points (denoted by solid circles).

(H) phases, which all join at the critical point at $\chi_C = 3/4$, $\mu = \Phi = 0$. (In three dimensions, one expects additional cubic phases, which are not studied here.) For larger values of χ, the H and L phases each terminate at a triple point, whereas experimentally one sees that these modulated phases exist even for very large values of χ. This unphysical part of the phase diagram is due to a breakdown of the gradient expansion in (1).

We first present results for grain boundaries in lamellar phases, and begin with the asymmetric tilt grain boundary (GB) between two perpendicular L phases. This is the *T-junction* of Ref. [2(b)], for which the layer continuity between the two adjoining phases is disrupted. Figures 2(a)–2(c) show order-parameter profiles ϕ for different χ and $\mu = 0$ (symmetric stripes), while Figs. 2(d)–2(f) show profiles for varying chemical potentials μ and $\chi = 1$ (asymmetric stripes). Figure 2(b) clearly shows the enlarged end caps noted in experiment [1,2], and the series 2(a)–2(c) predicts that they become less pronounced with increasing χ. The GB interfacial energy γ_{GB} scales as $\gamma_{GB} \sim (\chi - \chi_C)^{\mu_*}$ with $\mu_* = 3/2$,

Fig. 2(g), in accord with mean-field predictions [11]. To demonstrate that the interfacial energy γ_{GB} is indeed quite small, we show, with a dashed line, the difference in bulk free energies between the disordered and lamellar phases multiplied by one wavelength of the latter. This is roughly the cost per unit area of disordering such a width of lamellar phase. Clearly, the actual grain boundary bridges the two grains in a manner much less expensive than the insertion of a region of disorder. In Fig. 2(h) we plot the interfacial energies of two distinct GB structures, which are degenerate at $\mu = 0$, being related by order-parameter reflection symmetry $\phi \to -\phi$. For $\mu \neq 0$ this symmetry is broken, and the two structures correspond to distinct local free energy minima, one metastable and the other globally stable. The free-energy barriers between such interfacial structures are responsible for slow interface motion and, thus, long healing times in multigrain lamellar samples [12].

In Figs. 3(a)–3(c) we show symmetric tilt-boundary (TB) configurations for a fixed angle $\theta = 90°$ between the layer normals as a function of χ. Here the layer continuity is maintained across the boundary, and the *chevron* morphology is quite evident. In Figs. 3(d)–3(f), the tilt
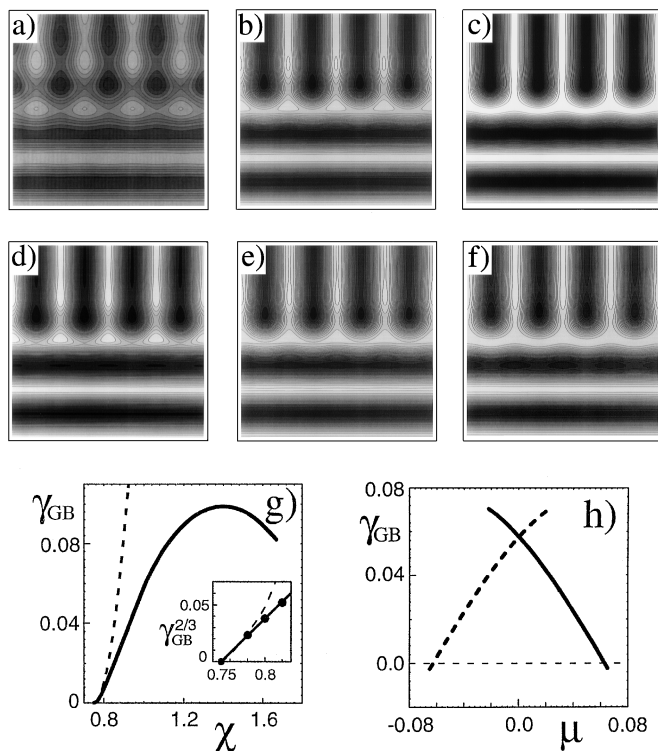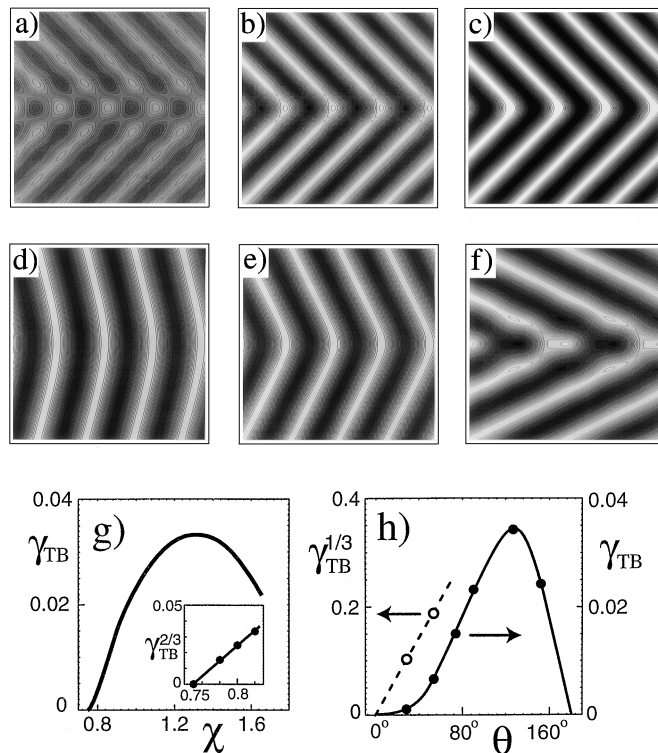

FIG. 2. Grain boundary (GB) between two perpendicular lamellar phases. (a)–(c) Contour plots of the order parameter profiles for $\mu = 0$ and $\chi = 0.78, 1, 1.5$; throughout the article the order parameter range $[-1, 1]$ is represented by 20 gray scales. (d)–(f) Profiles for $\chi = 1$ and $\mu = -0.02, 0.02, 0.06$. (g) GB interfacial energy γ_{GB} for $\mu = 0$ as a function of χ, showing asymptotic scaling with an exponent $\mu_* = 3/2$ (inset). The dashed line gives the surface free energy density of one lamellar layer for comparison. (h) γ_{GB} for $\chi = 1$ as a function of μ for two GB configurations which are degenerate at $\mu = 0$, but distinct otherwise.

FIG. 3. Tilt boundary (TB) between two lamellar phases. (a)–(c) Profiles for $\mu = 0$, a fixed angle $\theta = 90°$ between the layer normals, and $\chi = 0.78, 1, 1.5$. (d)–(f) Profiles for $\mu = 0$, $\chi = 1$, and $\theta = 28.08°, 53.14°$, and $126.86°$. (g) TB interfacial energy γ_{TB} for $\mu = 0$ as a function of χ, showing asymptotic scaling with an exponent $\mu_* = 3/2$ (inset). (h) γ_{TB} for $\chi = 1$ as a function of θ, showing a $\gamma_{TB} \sim \theta^3$ behavior for small θ (dashed line) and linear behavior for $\theta \to 180°$.

angle is progressively increased at fixed χ, and one clearly sees the change from the chevron to the *omega* structure. The omega shape of the layers at the boundary results from frustration due to an imposed local lamellar wavelength much larger than the equilibrium value. Figures 3(d)–3(f) resemble micrographs of undulating lamellar patterns in garnet films [13], and the similarity of Fig. 3(f) to the micrographs [2(b)] of diblock copolymer TBs is striking. The scaling of the TB energy γ_{TB} is again described by an exponent $\mu_* = 3/2$ [Fig. 3(g)]. Close to criticality, one finds pronounced reconstruction in terms of a square-like modulation, Fig. 3(a). For small θ, $\gamma_{TB}(\theta) \sim \theta^3$, Fig. 3(h), in accord with the bending behavior of elastic sheets; the $\theta \to 180°$ limit is expected to be linear, $\gamma_{TB}(\theta) \sim 180° - \theta$, in accord with a description in terms of decoupled dislocations of finite creation energy.

We now turn to interfaces between thermodynamically distinct phases. Interfacial structures between coexisting lamellar and disordered phases for three different values of the angle ϑ between the lamellae and the interface are shown in Figs. 4(a)–4(c) for $\chi = 1$ (where the phases and, therefore, also the interfacial structure are *metastable*), and in 4(d)–4(f) for $\chi = 1.5$ (where they

are stable). The metastable L-D boundary is shown as a dashed line in Fig. 1(b). In Figs. 4(a) and 4(d), for $\vartheta = 0°$, there is a relaxation of the outermost layers as the interface is approached, leading to a small increase in the wavelength, as in solids.

Before presenting the interfacial free energies, we describe our method of obtaining them because the calculation of such free energies between coexisting phases which can be modulated is nontrivial [14]. We calculate the total free energy, F^I, of phase I in a box employing periodic boundary conditions parallel to the left and right faces, and reflecting (Dirichlet) boundary conditions on those faces themselves. We adjust the length of the box so that the free-energy density is minimized. This occurs when the length of the box is some integer number of wavelengths of the periodic structure of phase I. The volume of the box is V'. By this means, there is *no* surface contribution to the total free energy, so that the bulk free energy is obtained directly; $f_b^I = F^I(V')/V'$. In a similar way we obtain $f_b^{II} = F^{II}(V'')/V''$. For the system in I, II coexistence, we calculate the total free energy in a box large enough that the order parameters attain their bulk values on the left and right faces at which reflecting boundary conditions are employed, and we vary the length of the box to minimize the interfacial excess free energy. The volume of the box is V. Again, there are no surface contributions so that we obtain $F^{I,II}(V,A) = V(f_b^I + f_b^{II})/2 + A\gamma_{I,II}$. As the bulk free energies are known, the desired interfacial energy follows directly.

The interfacial energy γ_{LD} is shown in Fig. 4(g). As χ is decreased, the coexistence between L and D is preempted by the hexagonal phase [see Fig. 1(b)]. This is manifest in the behavior of γ_{LD} for $\vartheta = 90°$ [dashed line in Fig. 4(g)] which becomes negative. This value of γ_{LD} is obtained by assuming an interfacial reconstruction locally resembling the energetically preferred hexagonal phase [see Fig. 4(c)]. The value of γ_{LD} for $\vartheta = 0°$ [solid line in Fig. 4(g)] remains positive down to $\chi \simeq 0.82$ and vanishes there with the classical tricritical exponent $\mu_* = 2$ [15]. Strong anisotropy of γ_{LD} as function of ϑ is observed [Fig. 4(h)], from which the shape of lamellar droplets in an isotropic phase can be qualitatively inferred: For $\chi > 1.34$ the drops are elongated parallel to the lamellae; for $\chi < 1.34$ the L and D phases are metastable at coexistence and the drops are elongated perpendicular to the lamellae.

Hexagonal-disordered interfacial structures are depicted in Figs. 5(a)–5(c); the corresponding interfacial energy γ_{HD}, shown in Fig. 5(g), scales again with $\mu_* = 2$. Structures for the hexagonal-lamellar interface are plotted in Figs. 5(d)–5(f), where we chose the mutual orientation in accord with the epitaxial relationship found for amphiphilic systems [16]. The corrugation of the lamellae near the interface, particularly evident in Fig. 5(d), resembles that seen in experiments on diblock copolymer blends
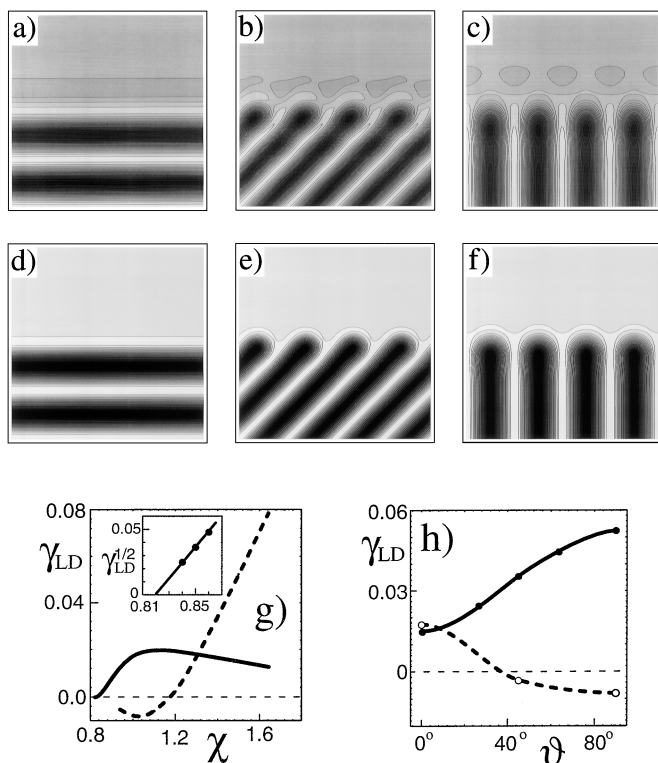

FIG. 4. Lamellar-disordered interface. (a)–(c) Profiles for $\chi = 1$ and different angles $\vartheta = 0°$, 45°, and 90° between the lamellae and the interface. (d)–(f) Profiles for $\chi = 1.5$. (g) Interfacial energy γ_{LD} for $\vartheta = 90°$ (dashed line) and $\vartheta = 0°$ (solid line), the latter scaling with $\mu_* = 2$ on approach to the metastable tricritical point (inset). (h) γ_{LD} as a function of the angle ϑ for $\chi = 1$ (dashed line) and for $\chi = 1.5$ (solid line).
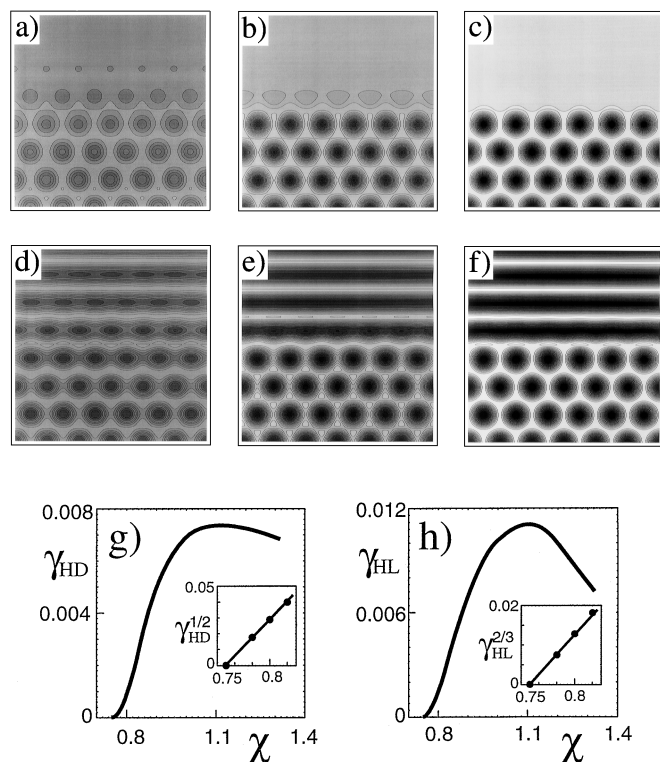
FIG. 5. (a)–(c) Hexagonal-disordered interfacial profiles for $\chi = 0.78$, 0.9, and 1.2. (d)–(f) Hexagonal-lamellar profiles for $\chi = 0.78$, 0.9, and 1.2. (g) Interfacial energy γ_{HD} along HD coexistence as a function of χ, scaling with $\mu_* = 2$ (inset). (h) γ_{HL} as a function of χ, scaling with $\mu_* = 3/2$ (inset).

[17]. The interfacial free energy of this interface, γ_{HL}, is plotted in Fig. 5(h) and scales with the classical critical exponent $\mu_* = 3/2$. This reflects the fact that, in contrast to the L-D and H-D interfaces, the H and L phases are locked into a fixed relative position with respect to translations perpendicular to the H-L interface.

At the triple point between disordered, lamellar, and hexagonal phases, $\chi \simeq 1.34$, we find $\gamma_{LD} > \gamma_{HL} + \gamma_{HD}$. It follows that the L-D interface that we have calculated is not the thermodynamically stable one. Within our model, the L-D interface is therefore wetted by the hexagonal phase at the triple point. As the occurrence of such points between these three phases is not uncommon experimentally [18], it would be interesting to determine whether this wetting does indeed occur.

Density fluctuations will decrease the interfacial critical exponent to a value $\mu_* < 3/2$, but leave the classical tricritical exponent $\mu_* = 2$ intact [11], while fluctuations of the direction of the modulation normals will eliminate the critical point [19]. By introducing uniaxiality, these latter fluctuations can be suppressed.

In summary, we have employed a simple Ginzburg-Landau free-energy functional to calculate profiles and free energies of several interfaces of modulated phases. Qualitative agreement with experiment is very good. The observed chevron and omega morphologies at lamellar grain boundaries emerge naturally, as do the expanded end caps, characteristic of the T-junction. We also calculated profiles and free energies of interfaces between disordered and modulated phases, and between modulated phases of different symmetry. In all but the simplest cases, there is significant reconstruction which leads to low interfacial energies. An extreme example of such reconstruction is the lamellar-disordered interface, which we find to be wetted by the hexagonal phase at an L-H-D triple point.

[1] M. Seul and D. Andelman, Science **267**, 476 (1995).
[2] (a) S. P. Gido, J. Gunther, E. L. Thomas, and D. Hoffman, Macromolecules **26**, 4506 (1993); (b) S. P. Gido and E. L. Thomas, Macromolecules **27**, 6137 (1994).
[3] Y. Nishikawa *et al.,* Acta Polym. **44**, 192 (1993); T. Hashimoto, S. Koizumi, and H. Hasegawa, Macromolecules **27**, 1562 (1994).
[4] E. Helfand and Y. Tagami, J. Chem. Phys. **56**, 3592 (1972); L. Leibler, Macromolecules **15**, 1283 (1982); A. N. Semenov, Sov. Phys. JETP **61**, 733 (1985).
[5] T. Garel and S. Doniach, Phys. Rev. B **26**, 325 (1982).
[6] D. Andelman, F. Brochard, and J.-F. Joanny, J. Chem. Phys. **86**, 3673 (1987).
[7] G. Gompper and M. Schick, Phys. Rev. Lett. **65**, 1116 (1990).
[8] L. Leibler, Macromolecules **13**, 1602 (1980); G. H. Fredrickson and E. Helfand, J. Chem. Phys. **87**, 697 (1987).
[9] G. H. Fredrickson, Macromolecules **20**, 2535 (1987).
[10] M. S. Turner, M. Rubinstein, and C. M. Marques, Macromolecules **27**, 4986 (1994).
[11] J. S. Rowlinson and B. Widom, *Molecular Theory of Capillarity* (Oxford University Press, New York, 1982).
[12] Similar local free-energy minima for a moving interface had been postulated in the context of crystal growth [J. W. Cahn, Acta Metall. **8**, 554 (1960)].
[13] M. Seul and R. Wolfe, Phys. Rev. Lett. **68**, 2460 (1992); Phys. Rev. A **46**, 7519 (1992).
[14] This problem has been formulated within the context of coexisting lamellar phases [A. Chatterjee and B. Widom, Mol. Phys. **80**, 741 (1993)]; B. Widom, KNAW Symposium, Amsterdam, 1994 (to be published).
[15] B. Widom, Phys. Rev. Lett. **34**, 999 (1975); see also Chap. 9.5 of Ref. [11].
[16] Y. Rancon and J. Charvolin, J. Phys. Chem. **92**, 6339 (1988); K. M. McGrath, P. Kékicheff, and M. Kĺeman, J. Phys. II (France) **3**, 903 (1993).
[17] R. J. Spontak *et al.,* Macromolecules **29**, 4494 (1996).
[18] For an example, see R. Strey, Ber. Bunsen-Ges. Phys. Chem. **97**, 742 (1993).
[19] S. A. Brazovskii, Sov. Phys. JETP **41**, 85 (1975).